



INTERNATIONAL JOURNAL OF ENGINEERING SCIENCES & RESEARCH TECHNOLOGY

ANALYSIS OF MICROCHANNEL HEAT SINK USING CFD

Vinod U.Patel *, Ashish J.Modi

* Assistant Professor, CGPIT Bardoli, Gujarat
Assistant Professor, GEC Bhuj, Gujarat

ABSTRACT

Investigations have been done to better understand the fluid flow and heat transfer in copper-based microchannel heat sinks designed for applications in electronics cooling. The present work addresses electronic chips cooling with force convection of alumina-water in copper based single microchannel heat sink by CFD software FLUENT. The Nusselt number variation along the flow direction is presented and compared for three different flow rates. The convection heat transfer coefficient also presented for above three cases. The laminar flow is considered during simulation along with energy equation. The different pressure drops are taken into consideration during simulation. The maximum pressure difference can be taken for more flux condition imposed on the boundary and also to suppress the rise of temperature of microchannel heat sink. The temperature rise of the heat sink for 10kPa, 20kPa, 35kPa, 50kPa and 65kPa are found to 398.7K, 342.5K, 321.6K, 313.9K and 308.5K respectively for copper microchannel heat sink when the heat flux is in the order of $9 \times 10^5 \text{ W/m}^2$.

KEYWORDS: Copper based Microchannel heat sink, CFD(Computational fluid dynamics).

INTRODUCTION

For thermal management of the high heat fluxes found in microelectronic devices, microchannels are the most effective at heat removal. The possibility of integrating microchannel directly in to the heat generating substrates makes them particularly attractive. The two important objectives in electronics cooling, reduction of substrate temperature gradients and minimization of the maximum substrate temperature can be achieved by the use of microchannel. Studies on microchannel flows in the past decade are categorized into various topics such as temperature, heat transfer in microchannel, investigation of single phase and two-phase flows in microchannel, minichannels and small tubes and Nusselt number, heat flux, comparison with flow in conventional channels gas flow in microchannels, analytical studies on microchannel flows and design and testing of microchannel heat sinks for electronics cooling.

Hetsroni et al. [1] Two-Phase Flow Patterns in Parallel Microchannels was studied by Hetsroni et al. [2]. They analysed the effect of geometry on flow and heat transfer, finding that an increasingly uniform heat flux resulted in an increased irregularity of temperature distribution on the chip surface Culham et al. [3] presented an analytical approach for characterizing electronic packages, based on the steady-state solution of the Laplace equation for general rectangular geometries, where boundary conditions are uniformly specified over specific regions of the package. Davies et al. [4] presented the method to correct the thermal resistance of electronics components is to adjust the junction-to-ambient thermal resistance to account for operational conditions. For forced convection applications, they proposed two factors; the first accounts for any upstream aerodynamic disturbance and the second addresses purely thermal interaction. Pucha et al. [5] presented a field-use induced damage mapping methodology that can take into consideration the field-use thermal environment profile to develop accelerated thermal cycling guidelines for packages intended to be used in military avionics thermal environment. Zhao and Lu [6] presented an analytical and numerical study on the heat transfer characteristics of forced convection across a microchannel heat sink. Two analytical approaches are used by them: the porous medium model and the fin approach. In the porous medium approach, the modified Darcy equation for the fluid and the two-equation model for heat transfer between the solid and fluid phases are employed. Chen et al. [7] developed an effective method for predicting and optimizing the thermal performance of heat sinks with Parallel-Plain fin under a given design constraint of pressure drop. They developed the thermal and hydrodynamic performance analyzers for PPF heat sinks. Fedorov and Visakanta [8] Modelling of transport in microchannels can be divided in to two categories. In the

[http:// www.ijesrt.com](http://www.ijesrt.com) © *International Journal of Engineering Sciences & Research Technology*

first, method used for macro-scale channels are directly implemented to evaluate the performance of microchannel heat sinks. H.A. Mohammed et al [9] investigated the impact of various nanofluid types on triangular microchannels heat sink cooling performance. In this study, an aluminium MCHS performance is examined using water as a base fluid with different types of nanofluids such Al_2O_3 , Ag, diamond- H_2O CuO , SiO_2 and TiO_2 as the coolants with nanoparticles volume fraction of 2%. Tsung-Hsun et al [10] investigated the MCHS performance using nanofluid as a coolant is examined. Two kinds of nanofluids, $\text{Cu}-\text{H}_2\text{O}$ and $\text{CNT}-\text{H}_2\text{O}$ are employed in this study. The MCHS structure is modelled as the porous medium and two-equation model are employed to describe the fluid and heat transfer in the MCHS. Roy and Bandyopadhyay [11] conducted a similar type investigation by developing a fully explicit twodimensional incompressible laminar Navier-Stokes solver in primitive variable formulation using a Cartesian staggered grid. Li et al. [12] numerically simulated a forced convection heat transfer occurring in silicon based micro channel heat sinks has been conducted using a simplified three-dimensional conjugate heat transfer model

MATHEMATICAL MODEL

The three-dimensional heat transfer and fluid flow in a rectangular microchannels heat sink are analyzed using water as the cooling fluid. A schematic of the structure of a rectangular microchannel heat sink as shown in Fig. 1. The micro-heat sink model made of a 10 mm long ($L=10$ mm) copper wafer having a depth of $h = 180 \mu\text{m}$, a width of $w = 57 \mu\text{m}$, and are separated by $43 \mu\text{m}$ wall thickness. A uniform heat flux is applied at the bottom of the heat sink. Heat transferred in the unit cell is a conjugate problem which combines heat conduction through the solid and dissipated away by convection of the cooling fluid in microchannel heat sink.

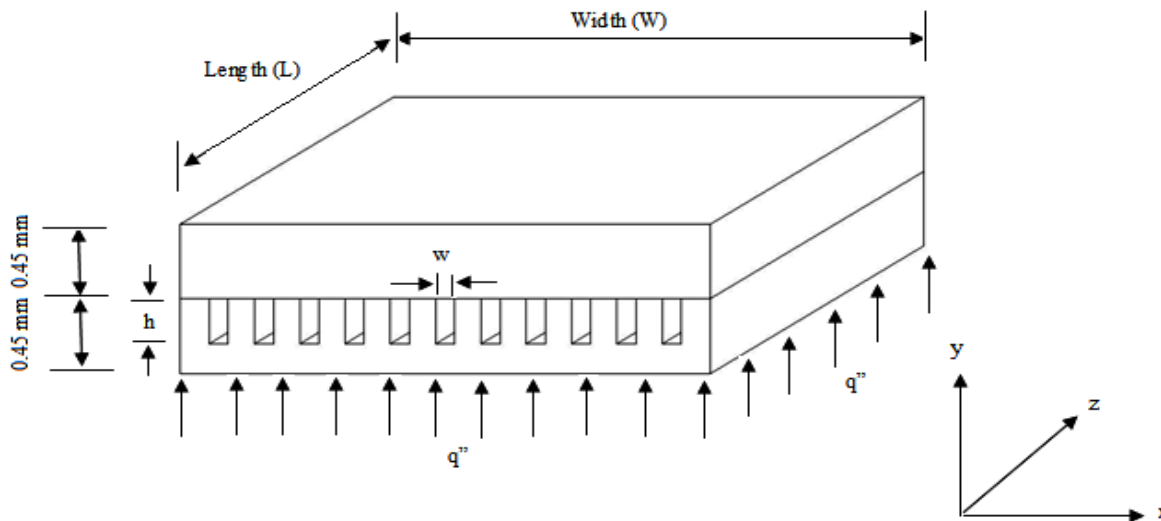


Fig.1 Schematic of microchannel heat sink

The bottom surface of heat sink at $y = 0$ is uniformly heated with a constant heat flux and at the top surface at $y = H$ is well insulated. The adiabatic conditions are applied at the other boundaries. Fluid flowing through the microchannel at temperature 293 K on account of pressure loss of 50 kPa. The direction of the fluid flow parallel to the z -axis as shown in Fig.2. The flow is assumed to be laminar and both hydrodynamically and thermally fully developed. The thermo physical properties are assumed to be constant.

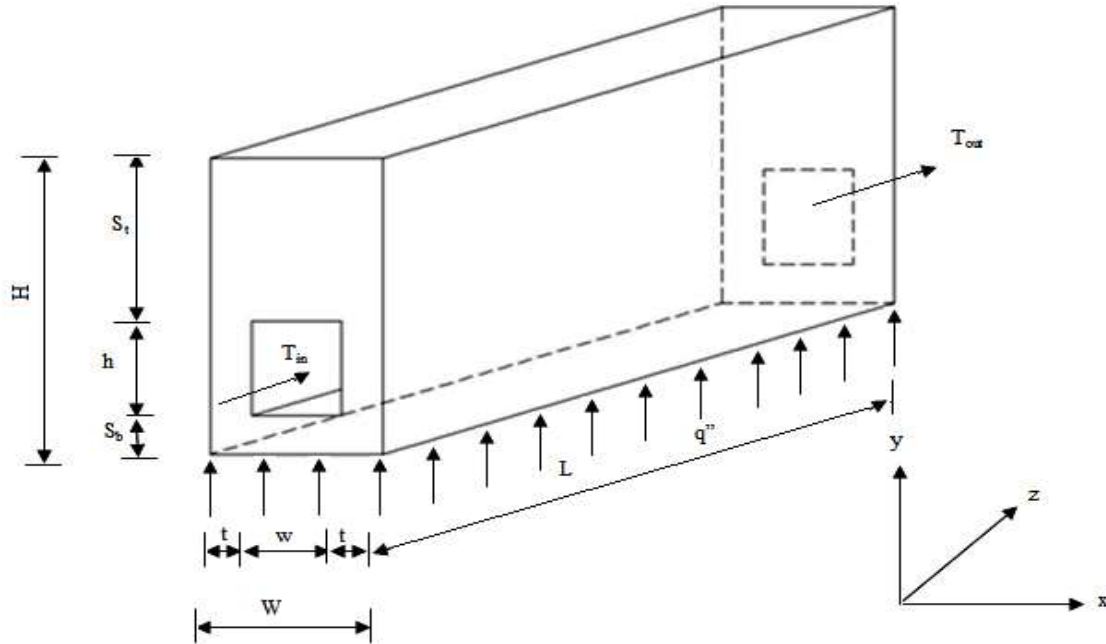


Fig.2 Computational domain of microchannel heat sink

SIMULATION OF MICROCHANNEL HEAT SINK

The meshed and boundary assigned domain is exported to the fluent as mesh file. The 3-d solver is selected. The grid is checked and smoothed after proper scaling of the domain. The material and boundary conditions are selected from fluent database. The solver for laminar flow is selected for simulation purpose. The energy equation, operating conditions are also imposed. The simulation starts from the heat flux boundary with gravity along y-direction. The second order upwind scheme is used to solve the combined convection diffusion effect in the governing equations. The SIMPLE algorithm was then applied to solve the coupled systems of equations. These conservation equations and boundary conditions can be stated in generalized forms as listed below:

Continuity equation

$$\frac{\partial u}{\partial x} + \frac{\partial v}{\partial y} + \frac{\partial w}{\partial z} = 0 \tag{1}$$

Momentum equation (Navier-stokes equation)

X-momentum equation

$$\rho(u \frac{\partial u}{\partial x} + v \frac{\partial u}{\partial y} + w \frac{\partial u}{\partial z}) = -\frac{\partial p}{\partial x} + \mu (\frac{\partial^2 u}{\partial x^2} + \frac{\partial^2 u}{\partial y^2} + \frac{\partial^2 u}{\partial z^2}) \tag{2}$$

Y-momentum equation

$$\rho(u \frac{\partial v}{\partial x} + v \frac{\partial v}{\partial y} + w \frac{\partial v}{\partial z}) = -\frac{\partial p}{\partial y} + \mu (\frac{\partial^2 v}{\partial x^2} + \frac{\partial^2 v}{\partial y^2} + \frac{\partial^2 v}{\partial z^2}) \tag{3}$$

Z-momentum equation

$$\rho(u \frac{\partial w}{\partial x} + v \frac{\partial w}{\partial y} + w \frac{\partial w}{\partial z}) = -\frac{\partial p}{\partial z} + \mu (\frac{\partial^2 w}{\partial x^2} + \frac{\partial^2 w}{\partial y^2} + \frac{\partial^2 w}{\partial z^2}) \tag{4}$$

Boundary conditions

For a steady, fully developed laminar flow $\frac{\partial u}{\partial x} = 0, v=0, w=0$. If the whole unit cell is chosen as a unitary domain, the boundary conditions can be specified as follows.

Hydrodynamic boundary conditions

The velocity is zero at all boundaries except the channel inlet and outlet.

1. At the inner bottom wall surface of channel (no-slip condition)
 $u = 0, v = 0, w = 0$

$$\text{For } y = S_b, t < x < t + w \tag{5}$$

2. At inlet $P_1 = P_{in}, v = 0, w = 0$

$$\text{For } z = 0, t < x < t + w \text{ and } S_b < y < S_b + h \tag{6}$$

3. At outlet $P_1 = P_{out}$

$$\text{For } z = L, t < x < t + w \text{ and } S_b < y < S_b + h \tag{7}$$

Thermal boundary conditions

Adiabatic boundary conditions are applied to all the boundaries of the solid region except the heat sink bottom wall, where a constant heat flux is applied.

1. $-k_s \frac{\partial T}{\partial y} = q''$
 $0 < z < L, 0 < x < W \text{ and } y = 0$ (8)

2. At inlet, the liquid temperature is equal to a given constant inlet temperature.

$$T = T_{in}$$

$$\text{For } z = 0, t < x < t + w \text{ and } S_b < y < S_b + h \tag{9}$$

3. The flow is assumed to be thermally fully developed at the channel outlet.

$$\frac{\partial^2 T}{\partial z^2} = 0$$

$$\text{For } z = L, t < x < t + w \text{ and } S_b < y < S_b + h \tag{10}$$

The hydraulic diameter is calculated as below:

$$D_h = \frac{4A}{\Gamma} = \frac{4hw}{2(h+w)} \tag{11}$$

Table 1 Thermophysical Properties of fluid

Fluid	ρ_f kg/m ³	k_f W/m-K	μ_f kg/m-s	C_p J/kg-K	T K
Water	998.2	0.6	0.001003	4182	293
Alumina-water (nanofluid) ($\phi=2.5\%$)	1072.5	0.658	0.001066	3865.79	293

Table 2 Thermophysical Properties of solid

Solid	ρ_s kg/m ³	k_s W/m-K	C_p J/kg-K
Silicon	2330	148	712
Copper	8978	381	387.6

Table 3 Relaxation factors

Pressure	0.3
Density	1
Momentum	0.7
Body force	1

Table 4 Flow conditions for microchannel heat sink

Sink Material	Δp (Pascal)
Copper	10000
	20000
	35000
	50000
	65000

RESULTS AND DISCUSSION

The model of the present study is validated using average heat transfer coefficient inside the channel for constant pressure drop 50 kPa and heat flux 90 W/cm² as shown in Fig.3. The result yield good agreement with the numerical results. It is significant that the present model demonstrates a better agreement with the numerical results in the average heat transfer coefficient compared to the model developed in J Li’s numerical work. The significant improvement of accuracy results given by the model in the present study is due to increase of density of grid system.

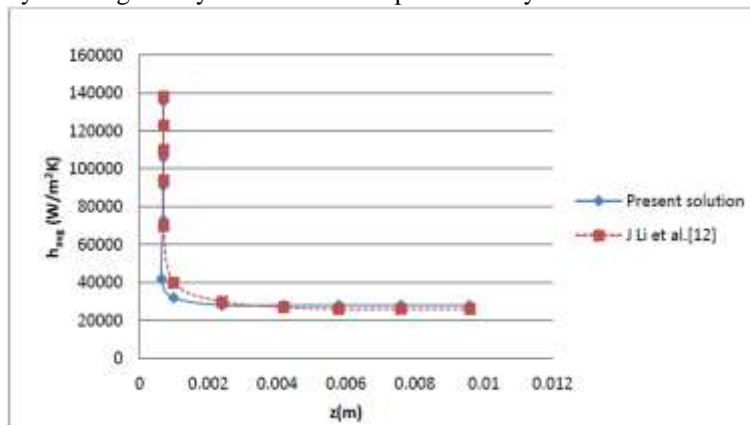


Fig.3 Model Validation

The fluid is entered through the microchannel at pressure 50 kPa with constant inlet temperature 293 K. After passing through the channel, the fluid discharged to the atmosphere i.e. gauge pressure. A constant heat flux $q'' = 90$ W/cm² applied at the bottom wall of heat sink and heat is absorbed by the alumina-water. The pressure contours inside channel as shown in Fig.4. Pressure of liquid is going to increases as the distance increases because of heat transfer occurs between wall and liquid in to the microchannel

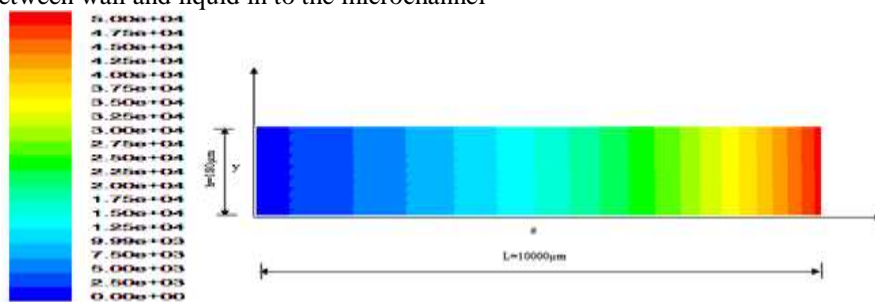


Fig.4 Pressure Contours of channel in y-z plane

The temperature of fluid at the inlet is initially uniform (293K). The temperature Profiles shown is due to the assumption of hydrodynamic fully developed Flow. The temperature rise along the flow direction in the solid and fluid regions of the microchannel heat sink. It is interesting to note that the temperature point is located at heated based surface of the heat sink as shown in Fig.5, which is immediately below the channel outlet. This is due to the low velocity of the fluid flow and resulting high concentration of heat flux.

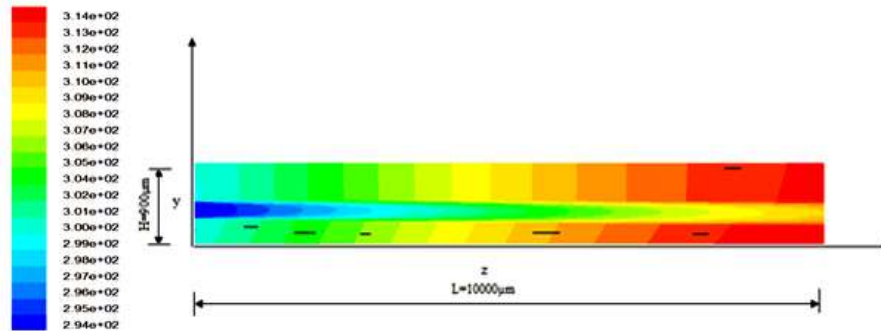


Fig.5 Temperature contours in y-z plane

The comparison of average liquid temperature variations inside the channel in x-y plane at 50 kpa, 20kpa and 10 kpa as shown in Fig.6.

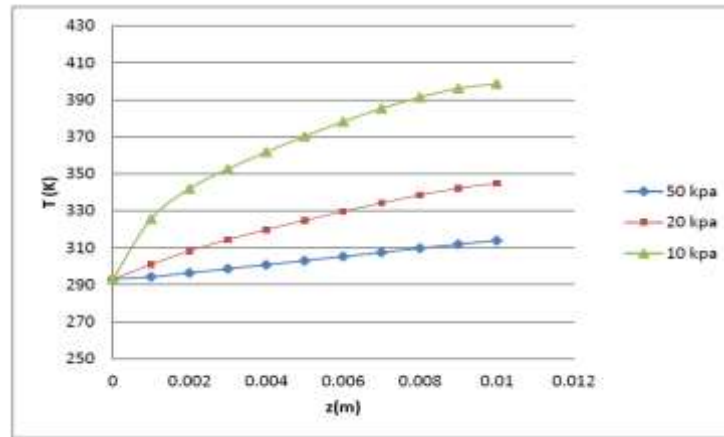


Fig.6 Average liquid temperature variations inside the channel in x-y plane for different pressure drops and $q'' = 90 \text{ W/cm}^2$

Fig.7 displays the velocity of the fluid at the outlet for 50 Kpa respectively. As the pressure difference decreases, the velocity decreases which is evident from the profiles at outlet.

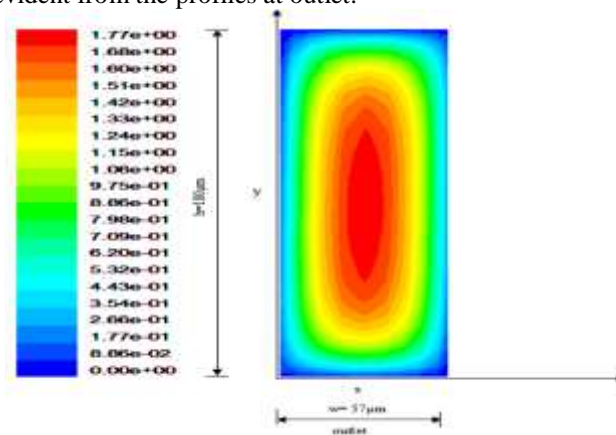


Fig.7 Velocity contour of channel in x-y plane for $\Delta p = 50 \text{ kPa}$ and $q'' = 90 \text{ W/cm}^2$

The average heat transfer coefficient sharply decreases at 1/10th of microchannel as shown in fig.8. For this the temperature of alumina-water is also found less at the entrance region and more at the exit of the channel. Due to growing boundary layer thickness, the heat transfer coefficient decreases along the flow direction and it is extremely high in the entrance region due to very thin local boundary layer. It decreases asymptotically to the fully developed value if the channel is sufficient long.

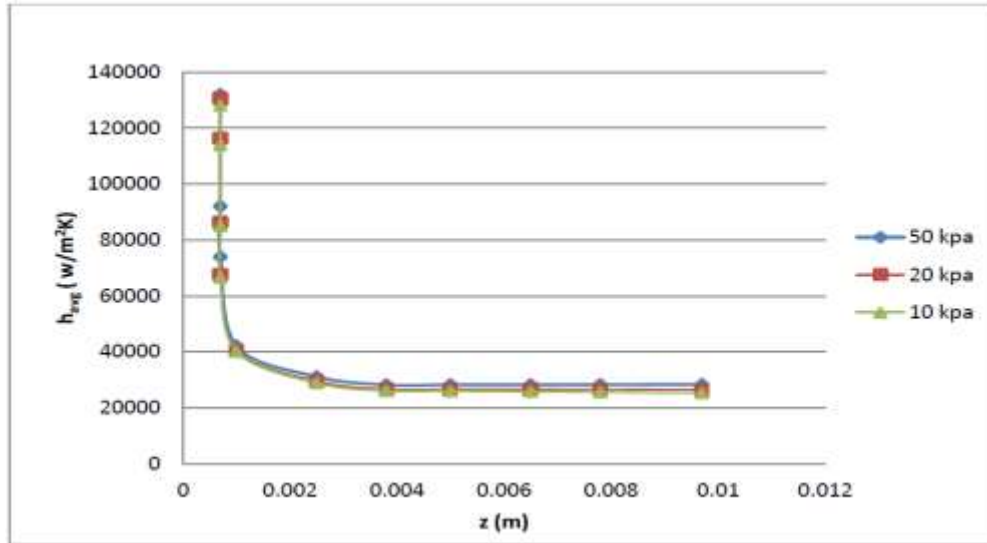


Fig.8 Average heat transfer coefficient distributions inside the channel in x-y plane for different pressure drop at $q'' = 90 \text{ W/cm}^2$

The average Nusselt number 3.7 obtained in case of $\Delta p = 50 \text{ kPa}$, lies between the values for a constant axial wall heat flux 4.8 and a constant axial wall temperature 4.0, for fully developed laminar flow in ducts, of rectangular cross-section with approximately $[w : h = 1 : 3 (57:180)]$. The average Nusselt number decreases along the channel due to formation of boundary layer and it is extremely high in the entrance region for different pressure drops (50, 20 and 10 kPa) due to very thin boundary layer as shown in Fig. 9.

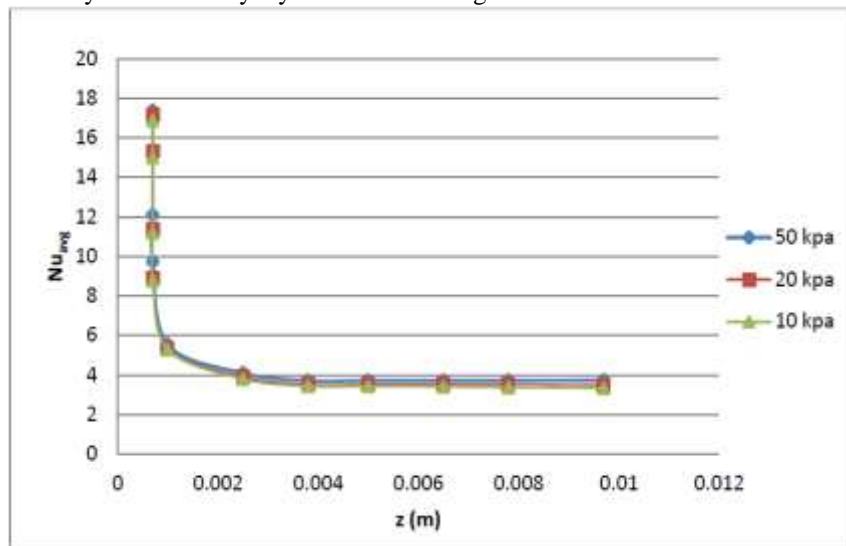


Fig.9 Average Nusselt number distributions inside the channel in x-y plane for different pressure drop at $q'' = 90 \text{ W/cm}^2$

CONCLUSION

1.The combined conduction–convection heat transfer in the microchannel produces very complex three-dimensional heat flow pattern with large, longitudinal, upstream directed heat recirculation zones in the highly conducting copper

substrate, where the fluid and solid are in direct contact. A detailed description of the average heat transfer coefficient, temperature, heat flux and Nusselt number was obtained.

2. The maximum temperature is located at heated base surface of heat sink, below the channel outlet. This is due to the low velocity of the fluid flow and resulting high concentration of heat flux.

3. The highest temperature is obtained at the channel outlet in case of 10 kPa at constant heat flux of 90 W/cm^2 , because of low velocity of fluid flow. As the heat flux increases, the outlet temperature goes on increasing because the fluid gets heated up more and more due to convective heat transfer. The maximum temperature of fluid rises in case of 10 kPa due to low liquid velocity and minimum temperature rises in case of 50 kPa due to high liquid velocity inside the microchannel at constant inlet temperature 313.9K .

4. The variations of the heat transfer coefficient and the Nusselt number along the flow direction is quite small for this type of microchannel heat sink after the thermal entrance lengths.

5. The average heat transfer coefficient, average Nusselt number variations decreases along the flow direction due to growing boundary layer thickness and extremely high at the entrance region due to the very thin local boundary layer. As the heat flux increase, the average heat transfer coefficient and average Nusselt number also increases for constant pressure drop.

6. The average heat fluxes from the solid to the coolant in the small inlet region of the microchannel are larger than those in the further downstream portion. This is because the average convective heat transfer coefficient is much larger in the upstream locations (the boundary layer thickness is small) and also because the highly conducting channel walls support very effective heat redistribution from the downstream (large convective resistance) to the upstream (small convective resistance) regions of the channel.

REFERENCES

- [1] Hetsroni, G., Mosyak, A. and Segal, Z., (2001), "Non-uniform temperature distribution), in electronic devices cooled by flow in parallel microchannels", IEEE Transactions on Components and Packaging technologies, Vol. 24, pp. 16-23..
- [2] Hetsroni, G., Mosyak, A., Segal, Z. and Pogrebnyak, E., (2003), "Two-phase flow patterns in parallel microchannels", International Journal of Multiphase Flow, Vol. 11, pp. 353-358..
- [3] Culham, J.R., Yovanovich, M.M. and Lemczyk, T.F., (2000), "Thermal characterization of electronic packages using a three-dimensional fourier series solution", ASME Journal of Electronic Packaging, Vol. 122, pp. 233-239.
- [4] Davies, M.R.D., Cole, R. and Lohan, J., (2000), "Factors affecting the operational thermal resistance of electronic components", ASME Journal of Electronic Packaging, Vol. 122, pp. 185-191.
- [5] Pucha, R.V., Tunga, K., Pyland, J. and Sitaraman, S.K., (2004), Accelerated thermal guidelines for electronic packages in military Avionics thermal environment", ASME Journal of Electronic packaging, Vol. 126, pp. 256-264.
- [6] Zhao, C.Y. and Lu, T.J., (2002), "Analysis of microchannel heat sinks for electronics cooling", international Journal of Heat and Mass Transfer, Vol. 45, pp. 4857-4869.
- [7] Chen, Han-Ting., Jenn-Tsong, Horng., Chen, Po-Li. and Hung, Ying- Huei., (2004), "Optimal design for PPF heat sinks in electronics cooling applications", ASME Journal of Electronic Packaging, Vol. 126, pp. 410-422.
- [8] Fedorov, A.G. and Viskanta, R., (2000), "Three-dimensional conjugate heat Transfer in the microchannel heat sink for electronics packaging", International Journal of Heat and Mass Transfer, Vol. 43, pp. 399-415.
- [9] H.A. Mohammed, P. Gunnasegaran and N.H. Shuaib, "The impact of various nanofluid types on triangular microchannels heat sink cooling performance", International Communications in Heat and Mass Transfer 38, 2011, pp.767-773.
- [10] Tsung-Hsun Tsai and Reiyu Chein, "Performance analysis of nanofluid-cooled microchannel heat sinks", International Journal of Heat and Fluid Flow 28, 2007, pp.1013-1026..
- [11] Roy, A. and Bandyopadhyay, G., (2004), "Numerical investigation of confined flow past a square cylinder placed in a channel", Journal of Institution of Engineers, Vol. 85, pp. 60-63. M. Weeks, Digital Signal Processing Using Matlab and Wavelets, Infinity Science Press LLC, 2007.
- [12] Li, J., Peterson, G.P. and Cheng, P., (2004), "Three-dimensional analysis of heat Transfer in a micro-heat sink with single phase flow", International Journal of Heat and Mass Transfer, Vol. 47, pp. 4215- 4231.

AUTHOR BIBLIOGRAPHY

[http:// www.ijesrt.com](http://www.ijesrt.com) © International Journal of Engineering Sciences & Research Technology

	<p>Vinod U.Patel Assistant Professor,CGPIT Bardoli,Gujarat Email: vinod.mech06@gmail.com</p>
	<p>Ashish J.Modi Assistant Prfessor,GEC Bhuj,Gujarat Email: ashishjmodi@gmail.com</p>